



HAL
open science

Ab initio calculations of collisional line–shape parameters and generalized spectroscopic cross-sections for rovibrational dipole lines in HD perturbed by He

K. Stankiewicz, Hubert Józwiak, M. Gancewski, N. Stolarczyk, Franck Thibault, Piotr Wcislo

► To cite this version:

K. Stankiewicz, Hubert Józwiak, M. Gancewski, N. Stolarczyk, Franck Thibault, et al.. Ab initio calculations of collisional line–shape parameters and generalized spectroscopic cross-sections for rovibrational dipole lines in HD perturbed by He. *Journal of Quantitative Spectroscopy and Radiative Transfer*, 2020, 254, pp.107194. 10.1016/j.jqsrt.2020.107194 . hal-02931935

HAL Id: hal-02931935

<https://hal.science/hal-02931935>

Submitted on 10 Sep 2020

HAL is a multi-disciplinary open access archive for the deposit and dissemination of scientific research documents, whether they are published or not. The documents may come from teaching and research institutions in France or abroad, or from public or private research centers.

L'archive ouverte pluridisciplinaire **HAL**, est destinée au dépôt et à la diffusion de documents scientifiques de niveau recherche, publiés ou non, émanant des établissements d'enseignement et de recherche français ou étrangers, des laboratoires publics ou privés.

Highlights

- Close-coupling calculations of generalized spectroscopic cross-sections
- Ab initio investigation of pressure broadening and shift coefficients
- Ab initio investigation of Dicke parameters
- Data for electric dipole R ($j=0-5$) and P ($j=1-6$) lines for purely rotational transitions, fundamental band and first four overtones

Journal Pre-proof

Highlights for *Ab initio* calculations of collisional line–shape parameters and generalized spectroscopic cross-sections for rovibrational dipole lines in HD perturbed by He by

Kamil Stankiewicz, Hubert Jóźwiak, Maciej Gancewski, Nikodem Stolarczyk, Franck Thibault, Piotr Wcisło

Highlights

- Close-coupling calculations of generalized spectroscopic cross-sections
- *Ab initio* investigation of pressure broadening and shift coefficients
- *Ab initio* investigation of Dicke parameters
- Data for electric dipole R ($j=0-5$) and P ($j=1-6$) lines for purely rotational transitions, fundamental band and first four overtones

Ab initio calculations of collisional line–shape parameters and generalized spectroscopic cross-sections for rovibrational dipole lines in HD perturbed by He

Kamil Stankiewicz^{a,*}, Hubert Jóźwiak^a, Maciej Gancewski^a, Nikodem Stolarczyk^a,
Franck Thibault^b, Piotr Wcisło^a

^a*Institute of Physics, Faculty of Physics, Astronomy and Informatics, Nicolaus Copernicus University, Grudziądzka 5, Toruń, 87-100, Poland*

^b*Univ Rennes, CNRS, IPR (Institut de Physique de Rennes)-UMR 6251, F-35000 Rennes, France*

Abstract

We report *ab initio* calculations of generalized spectroscopic cross-sections for hydrogen deuteride perturbed by helium. From these calculations, collisional line–shape parameters are deduced for the HD electric dipole transitions: from R(0) to R(5) and from P(1) to P(6) in the 0–0 to 5–0 bands. These parameters are necessary for a proper interpretation of HD spectra from the atmospheres of gas giants. We demonstrate that the centrifugal distortion cannot be ignored, not only for pure rotational lines but also for rovibrational lines when one aims at sub-percent accuracy of the collisional line–shape parameters.

Keywords: HD, He, line–shape parameters, molecular collisions, quantum scattering, complex Dicke parameter

1. Introduction

Molecular hydrogen is the most widespread molecule in the Universe. It is also the simplest molecule, the structure of which can be calculated from first principles, which makes it well suited for accurate tests of *ab initio* calculations. A mixture of molecular hydrogen and helium is the main component of the atmospheres of gas giants in the Solar System and is predicted to be a dominant constituent of the atmospheres of some exoplanets [1]. Despite its considerably smaller abundance compared to the H₂ isotopologue, HD is noticeable in spectroscopic studies due to the presence of electric dipole transitions, the intensities of which are much larger than the extremely weak quadrupole transitions in H₂. An accurate list of the line–shape parameters is necessary for a correct interpretation of molecular spectra from the atmospheres of gas giants [2] and exoplanets [3]. Studies of the H₂–rich atmospheres are well suited for measuring the D/H ratio, which is crucial for understanding the evolution of the Universe and planets’ atmospheres [4, 5].

The relevant collisional systems for spectroscopic studies of gas giants’ atmospheres that involve molecular hydrogen are: H₂–H₂, H₂–He, HD–H₂ and HD–He. The He–perturbed H₂ was thoroughly examined both theoretically [6–8] and experimentally [9]. The research program aiming at calculating the He–perturbed H₂ line–shape parameters was recently concluded with producing a comprehensive dataset of the beyond-Voigt line–shape parameters for this system that covers all the rovibrational transitions and a wide range of temperatures [10]. Several purely rotational transitions were recently investigated for He–perturbed HD in Ref. [11].

In this paper, we present fully *ab initio* calculations of the generalized spectroscopic cross-sections (GSXS) and collisional line–shape parameters for the HD molecule in helium bath. The GSXS were obtained by performing dynamical close-coupling calculations at various relative kinetic energies of the colliding pair using the most recent *ab initio* potential energy surface (PES) [7], which is an improved version of the one reported by Bakr, Smith and Patkowski PES [12] (we refer to it as BSP PES). The quantum scattering calculations were performed with the recently developed BIGOS com-

*Corresponding author

Email addresses: stankiewiczkamil198@gmail.com (Kamil Stankiewicz), piotr.wcislo@umk.pl (Piotr Wcisło)

puter code [13]. More specifically, the calculations
 were performed for selected $v_j \rightarrow v'_j$ rovibrational
 transitions from $v = 0$, $v' = 0$ to 5, $j = 0$ to 5
 for the R lines and $j = 1$ to 6 for the P lines. De-
 spite that there are no P lines for purely rotational
 transitions in the absorption spectrum, we report
 the line-shape parameters for them for complete-
 ness. We derive the pressure broadening and shift
 coefficients, as well as the real and imaginary parts
 of the Dicke parameter. The line-shape param-
 eters, at different temperatures, are obtained by av-
 eraging the GSXS over our grid of relative kinetic
 energies of the colliding pair.

2. Calculations

In this section, we briefly explain the methodol-
 ogy of our *ab initio* quantum scattering calculations
 used to obtain the GSXS and collisional line-shape
 parameters for the He-perturbed HD lines.

2.1. Generalized spectroscopic cross sections

The PES for H₂-He interaction, $V(r, R, \theta)$, de-
 pends on three parameters: r – the distance be-
 tween the protons in the hydrogen molecule, R –
 the intermolecular distance between the hydrogen
 molecule center of mass and helium atom, and θ –
 the angle between the molecular bonding axis
 and the axis connecting its center of mass with
 the helium atom. Since we work within the Born-
 Oppenheimer approximation, we can apply the H₂-
 He PES to the HD isotopologue by simply shifting
 the center of mass of the hydrogen molecule. The
 HD-He interaction PES is expanded over the Leg-
 endre polynomials:

$$V(r, R, \theta) = \sum_{L=0}^{L_{max}} V_L(r, R) P_L(\cos \theta). \quad (1)$$

Due to the small anisotropy of the PES, it is suffi-
 cient to truncate the expansion at $L_{max} = 7$ [11].
 Both odd and even terms of the expansion must be
 taken into account (in contrast to H₂ and D₂) since
 HD is a heteronuclear molecule. To solve the scat-
 tering equations we compute radial coupling terms:

$$V_{L, v, j, v', j'}(R) = \int_0^\infty \chi_{v', j'}(r) V_L(r, R) \chi_{v, j}(r) dr, \quad (2)$$

where $\chi_{v, j}(r)$ are the HD rovibrational wavefunc-
 tions. We neglect the vibrational coupling, hence

only $v = v'$ radial terms are considered in our cal-
 culations. It has been demonstrated in several arti-
 cles that for purely rotational lines it is important
 to take the centrifugal distortion into account [6–
 9, 11, 14, 15]. Disregarding the centrifugal distor-
 tion leads to the assumption that $j = j' = 0$ for
 all radial coupling terms. This approach is usually
 used in the case of rovibrational transitions [6–9].
 In this work, we show that the centrifugal distor-
 tion cannot be neglected for the rovibrational lines
 if one aims at sub-percent accuracy of the calcu-
 lated line-shape parameters.

The major part of the calculations consists of
 solving the close-coupling equations [16, 17]. The
 BIGOS code [13] solves the coupled equations in
 the body-fixed (BF) frame of reference,

$$\left[\mathbf{I} \frac{d^2}{dR^2} + k_\gamma^2 \mathbf{I} - \frac{1}{R^2} (\mathbf{L}^2)^{pJ} \right] \mathbf{F}^{pJ}(R) = 2\mu \mathbf{V}^{pJ}(R) \mathbf{F}^{pJ}(R), \quad (3)$$

for each pair of total angular momentum (J) and
 parity (p), using the renormalized Numerov's al-
 gorithm [18]. Here, $k_\gamma^2 = 2\mu(E - E_\gamma)$, E is the
 total energy of the system, E_γ is the energy of the
 rovibrational state, and μ is the reduced mass of
 the HD-He system. Numerical solution of Eq. (3)
 is found in the form of the log-derivative matrix
 $Y^{pJ} = F^{pJ}/F^{pJ}$, which is transformed to the
 space-fixed frame at sufficiently large value of R .
 The scattering matrix is obtained from the bound-
 ary conditions imposed on the wavefunction of the
 system [18]. The S-matrix is used to calculate the
 GSXS [19, 20]:

$$\begin{aligned} \sigma_\lambda^q(v_i, j_i, v_f, j_f; E_{kin}) &= \frac{\pi}{k^2} \sum_{J_i, J_f, l, l', \bar{l}, \bar{l}'}^\infty i^{l-l'-\bar{l}+\bar{l}'} \\ &\times (-1)^{l-l'-\bar{l}+\bar{l}'} [J_i] [J_f] \sqrt{[l] [l'] [\bar{l}] [\bar{l}']} \begin{pmatrix} l & \bar{l} & \lambda \\ 0 & 0 & 0 \end{pmatrix} \\ &\times \begin{pmatrix} l' & \bar{l}' & \lambda \\ 0 & 0 & 0 \end{pmatrix} \begin{bmatrix} j_i & j_i & \bar{l} & \bar{l}' \\ j_f & l & j_f & l' \\ q & J_f & J_i & \lambda \end{bmatrix} [\delta_{ll'} \delta_{\bar{l}\bar{l}'}] \\ &- \langle v_i j_i l' | \mathbf{S}^{J_i}(E_{T_i}) | v_i j_i l \rangle \langle v_f j_f \bar{l}' | \mathbf{S}^{J_f}(E_{T_f}) | v_f j_f \bar{l} \rangle^* \end{aligned} \quad (4)$$

The initial state of a transition is labeled by the
 v_i and j_i quantum numbers, and final by v_f and
 j_f . J_i and J_f are the initial and final total angu-
 lar momentum, respectively, l is the relative angu-
 lar momentum of the HD-He motion, k is the

wavenumber related to the initial kinetic energy.

105 Total energies of the system in the initial and final spectroscopic states are denoted by E_{T_i} and E_{T_f} , and are the sums of the kinetic energies and the energies of the rovibrational states. The symbol $[x]$ stands for $(2x+1)$, the matrices written in paranthesis are Wigner 3-j symbols and the matrix in square bracket is a Wigner 12-j symbol of the second type. Index q describes the rank of the radiation-matter interaction tensor. For dipole lines $q = 1$. For more details the reader is referred to Refs. [8] and [19]. The real and imaginary parts of $\sigma_{\lambda=0}^{q=1}$ are called pressure broadening (PBXS) and pressure shift (PSXS) cross-sections, respectively. $\sigma_{\lambda=1}^{q=1}$ is the complex Dicke cross-section. We refer to the real and imaginary parts of the Dicke cross-section as RDXS and IDXS, respectively.

2.2. Collision integrals and line shape parameters

The line-shape parameters are obtained by evaluating the collision integrals [19–21],

$$\omega_{\lambda}^{s s'}(q) = \langle v \rangle \int_0^{\infty} x^{(s+s'+2)/2} e^{-x} \sigma_{\lambda}^q dx, \quad (5)$$

where $\langle v \rangle = \sqrt{8k_B T / \pi \mu}$, σ_{λ}^q is the GSXS given by Eq. (4) and $x = E_{kin} / k_B T$; k_B , T and μ denote Boltzmann constant, temperature and reduced mass of the system, respectively. Speed-averaged pressure broadening and shift, Γ_0 and Δ_0 , and complex Dicke parameter, ν_{opt} , are related to Eq. (5) through [7, 22]

$$\Gamma_0 + i\Delta_0 = \frac{1}{2\pi c} \frac{p}{k_B T} \omega_0^{00}(q), \quad (6)$$

$$\nu_{opt} = \frac{1}{2\pi c} \frac{p}{k_B T} M_2 \left[\frac{2}{3} \omega_1^{11}(q) - \omega_0^{00}(q) \right], \quad (7)$$

where p is pressure, $M_2 = m_2 / (m_1 + m_2)$, with $m_{1/2}$ being masses of active/perturbing species, and c is the speed of light; normalization factor $(2\pi)^{-1}$ arises when one uses frequency instead of angular frequency to describe the spectrum.

We denote the gas density-normalized values of the line-shape parameters with their lowercase-letter counterparts, i.e., γ_0 and δ_0 , and $\tilde{\nu}_{opt}$ for the complex Dicke parameter. To compare our results with previous experiments, we provide the parameters in units of $\text{cm}^{-1}/\text{amagat}$.¹

¹The amagat (amg) is defined as the number of molecules of an ideal gas per unit volume at standard temperature and pressure conditions.

3. Results

In this section, we present the results of our *ab initio* calculations of the GSXS and line-shape parameters. We also discuss the influence of centrifugal distortion on the rovibrational lines.

3.1. Generalized spectroscopic cross sections

First, we discuss the dependence of the GSXS on the kinetic energy, vibrational band, and initial molecular rotational state. We plot only a part of the examined transitions. The full dataset for all the lines is provided in the supplementary material [23]. In the data files we also include the inelastic contribution to the pressure broadening cross-section (see Appendix A. of Ref. [6]).

Figure 1 shows the dependence of the PBXS and PSXS on the vibrational band for the lowest initial rotational quantum number for selected lines belonging to the R and P-branches. Figure 2 shows the PBXS and PSXS dependence on the initial rotational number for the fundamental band. We also present the inelastic contribution to the PBXS for each transition. The behavior of the PBXS and PSXS for the two branches is very similar. They exhibit similar dependencies of the cross-sections on the kinetic energy (K.E.). As expected, the PBXS for purely rotational lines R(0) and P(1) is the same, while the PSXS only differs by the sign. The same observation was made for all pairs of purely rotational lines R(j) and P(j+1) and was reported in multiple previous studies for S(j) and O(j+2) lines in H₂-He and D₂-He systems [8, 15, 24]. From 0.2 cm^{-1} the values of PBXS decrease, reach a minimum around energy 10–40 cm^{-1} and increase at higher energies. Near the minimum of the PBXS, at K.E. about 10–15 cm^{-1} , the PSXS changes its sign. The intuitive explanation of this has been presented in Ref. [8]. At low relative K.E. the de Broglie wavelength of the scattering system is relatively large, the long-range attractive part of the potential plays a significant role. At higher K.E., the repulsive part of the potential becomes more important. Because the shift results from the difference of scattering phase shifts, it may change its sign while passing from very low energies to higher ones. Finally, the cross-sections increase for higher energies because of the growing contribution from the inelastic collisions [6].

For the R_v(0) and P_v(1) lines a rapid change in both the PBXS and the inelastic contribution to the PBXS around 90 cm^{-1} can be observed. This

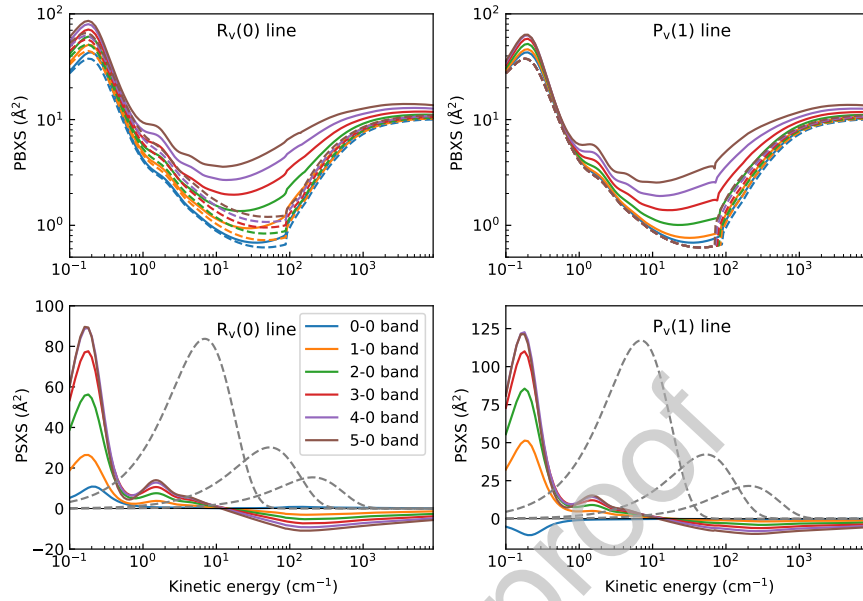


Fig. 1. R(0) and P(1) pressure broadening and shift cross-sections (PBXS and PSXS, respectively) for different vibrational bands as a function of the collision kinetic energy. The dashed lines in the upper panels represent the inelastic contribution to the PBXS for each transition. The dashed gray lines are the Maxwell-Boltzmann distributions at a temperature of 10 K, 77 K, and 296 K. PBXS and PSXS are the real and imaginary parts of $\sigma_{\lambda=0}^{q=1}$, respectively.

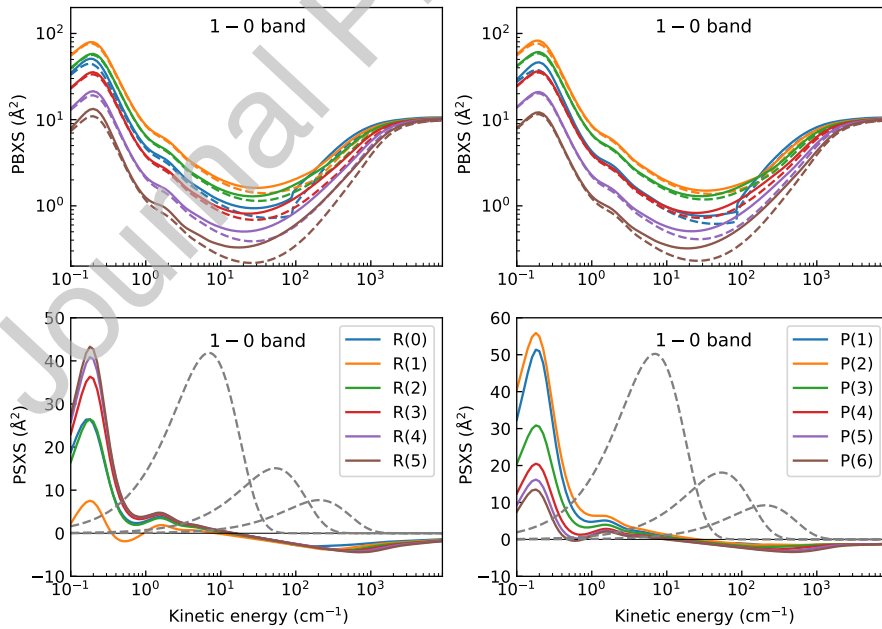


Fig. 2. PBXS and PSXS for different rotational transitions of the fundamental band as a function of collision kinetic energy. The dashed lines in the upper panels represent the inelastic contribution to the PBXS for each transition. The dashed gray lines are the Maxwell-Boltzmann distributions at the temperature of 10 K, 77 K, and 296 K.

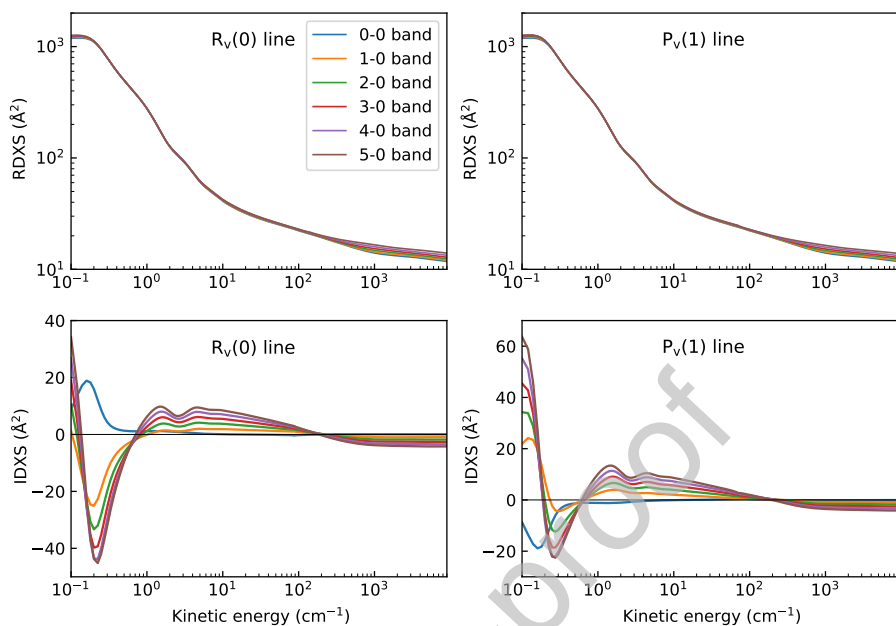


Fig. 3. The real and imaginary part of Dicke cross-sections $\sigma_{\nu}^{(0)}$ (RDXS and IDXS, respectively) for the R(0) and P(1) lines of different vibrational bands as a function of the collision kinetic energy.

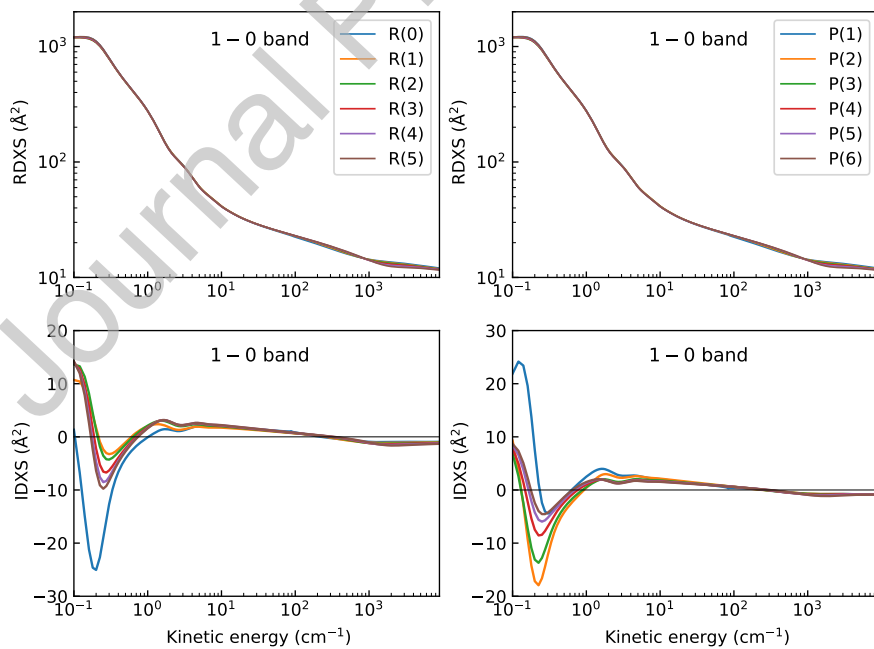


Fig. 4. The RDXS and IDXS for different rotational transitions of the fundamental band as a function of the collision kinetic energy.

is due to the fact that at this K.E. the first inelastic channel in the initial spectroscopic state ($v, j = 1$) becomes energetically accessible. Note that in the case of the $R_v(0)$ lines, this threshold energy corresponds to K.E. = 89 cm^{-1} since all these lines share the same initial spectroscopic state. However, one can observe that the larger the value of v is, the less significant is this rapid change in the PBXS. On the other hand, for $P_v(1)$ lines this threshold energy varies with v . This is because the inelastic contribution from the first open channel originates from the final spectroscopic state, and the rovibrational energy of the $E_{v,j=0}$ state varies from about 89 to 71 cm^{-1} , for the $v = 0$ and $v = 5$ states, respectively. The sharp change cannot be spotted for $R(j)$ and $P(j+1)$ for $j > 0$ because neither in the initial nor in the final state the molecule occupies the ground rotational level $j = 0$. Thus, there is always at least one inelastic channel open in both spectroscopic states, regardless of the K.E. considered. We note that the opening of the next inelastic channel causes a much weaker change in the cross-sections.

It can also be noticed in Fig. 1 that at low K.E. the inelastic contribution to the PBXS is identical for the $P_v(1)$ lines, while this contribution differs for the $R_v(0)$ lines. The inelastic contributions to the PBXS for $P_v(1)$ and $R_v(0)$ lines are defined as

$$\begin{aligned} \sigma_{PB_{inel}}[P_v(1)] &= \frac{1}{2} \left\{ \sum_{j' \neq 1} \sigma_{(v=0, j=1 \rightarrow v=0, j')} + \sum_{j' \neq 0} \sigma_{(v, j=0 \rightarrow v, j')} \right\} \\ \sigma_{PB_{inel}}[R_v(0)] &= \frac{1}{2} \left\{ \sum_{j' \neq 0} \sigma_{(v=0, j=0 \rightarrow v=0, j')} + \sum_{j' \neq 1} \sigma_{(v, j=1 \rightarrow v, j')} \right\}, \end{aligned}$$

where the σ denote standard state-to-state cross-sections. Both spectroscopic transitions involve the same rotational levels but in different vibrational states, thus the inelastic state-to-state cross-sections out of them are different. However, in the $P_v(1)$ case, at low kinetic energies only the state-to-state cross-section from $v = 0, j = 1$ to $v = 0, j = 0$ contributes; this contribution does not depend on v . When the kinetic energy reaches $E_{v, j=1} - E_{v, j=0}$, then the inelastic contribution coming from the upper state ($v = 1, j = 0$) starts to contribute; note that this threshold depends on v since the rotational spacing depends on the vibrational state. For the later, the $R_v(0)$ lines, the situation is reversed. At low kinetic en-

ergies only the state-to-state cross-section from $v, j = 1$ to $v, j = 0$ contributes and this cross-sections depends on v . The inelastic cross-sections out of $v = 0, j = 0$ start to contribute to the PBXS when the level $v = 0, j = 1$ is energetically accessible, at $E_{kin} = E_{v=0, j=1} - E_{v=0, j=0}$.

The values of the PBXS and absolute values of the PSXS distinctively increase with the vibrational band. A similar observation was made for the H_2 -He system in Ref. [8]. This is due to two factors. First, for the rovibrational bands, a significant part of the PBXS and PSXS comes from the rovibrational dephasing, which mainly results from the difference in the isotropic components of the PES for different v . For $v=0$ bands this difference increases with v . Secondly, the spacing between rotational energy levels decreases with increasing vibrational number. This enhances the inelastic processes which can be observed in Fig. 1.

Figure 2 presents the dependence of the PBXS and PSXS on the rotational quantum number j for the fundamental band. The PBXS generally decreases with increasing j . The only exceptions to this rule seem to be lines $R(0)$ and $P(1)$ for low energies. However, right above the energy threshold of the first inelastic channel, the PBXS significantly increases and surpasses the values of the PBXS for higher rotational numbers. As noticed in [8] the PBXS for low j is sensitive both to the long-range and short-range interaction while for higher j it is mostly sensitive to the short-range part of the PES. Moreover, for a given v the spacing between rotational levels increases with increasing j , which should impact the contribution from the inelastic collisions. The two factors explain the observed dependence on j . The PSXS does not display such monotonicity for lower energies, but it occurs for higher ones. Cross-sections for both branches hold similar dependence on the kinetic energy for different j and v . The PSXS also change their signs at nearly the same energy for all investigated lines.

Figures 3 and 4 present the dependence of the real and imaginary part of the Dicke cross-sections (RDXS and IDXS) on the rotational and vibrational number, respectively. As reported before in Refs. [7] and [8] for the He-perturbed H_2 , the dependence of the RDXS on v and j is marginal for low kinetic energies and can be only noticed for energies higher than around 200 cm^{-1} , which can be attributed to the increasing contribution from the inelastic collisions. We observe that the values of the RDXS slightly increase with the vibrational

quantum number v but the differences are much smaller than for the PBXS. For energies higher than 1000 cm^{-1} the RDXS slightly decreases with j . The dependence on v and j for IDXS is similar as for PSXS. The absolute values of the IDXS increase with increasing v . For higher energies, the IDXS decreases with j while for lower energies there is no monotonic dependence on the rotational number. The change of the sign is also observed, but for energies around 150–200 cm^{-1} . For purely rotational transitions R(j) and P($j+1$), the RDXS values are the same while the IDXS values change their sign. Such behavior was also reported in previous studies for S(j) and O($j+2$) lines in H_2 -He and D_2 -He systems [8, 15].

3.2. Line-shape parameters

In this subsection, we present the calculated collisional line-shape parameters: the pressure broadening coefficient, γ_0 , the pressure shift coefficient, δ_0 , and the real and imaginary parts of the Dicke parameter, $\tilde{\nu}_{opt}^r$ and $\tilde{\nu}_{opt}^i$, respectively. Calculations were conducted at 30 temperatures ranging from 5 to 2000 K. In this paper, we plot our results at a temperature of 296 K. The full data is provided in the supplementary material [23].

Figure 5 shows γ_0 and δ_0 for all examined lines. As noticed in the discussion on the GSXS, both γ_0 and δ_0 distinctly increase with the vibrational band essentially because the vibrational dephasing increases. δ_0 dependence on v seems to be non-linear, while γ_0 increases faster for higher bands. The dependence of γ_0 on j varies depending on the vibrational band which was also observed in the GSXS. For lower v , the pressure broadening coefficients decrease with j , while for higher v they increase with j . The pressure shift coefficients generally increase with j at this temperature except for the 0–0 vibrational band in the R-branch. While the dependence on j seems to be much more important with increasing v , the relative dependence of δ_0 does not change very sharply.

Figure 6 presents complex Dicke parameters for all studied lines. The real and imaginary parts of the Dicke parameter depend on j and v oppositely to γ_0 and δ_0 , respectively [25]. This behavior can be explained by the following relation (see Appendix A in Ref. [26])

$$\tilde{\nu}_{opt} = \left(\frac{2}{3}\right) M_2 \omega_1^{11} - M_2(\gamma_0 + i\delta_0). \quad (8)$$

In our case of He-perturbed HD, $M_2 \approx 4/7$. Note that, in general, the j and v dependence of $\tilde{\nu}_{opt}$ is dominated by the first term in Eq. (8), i.e., $(2/3)M_2\omega_1^{11}$. However, in the case of molecular hydrogen the situation is completely reversed and a major contribution comes from the second term in Eq. (8), $-M_2(\gamma_0 + i\delta_0)$, which is clearly seen when comparing Figs. 5 and 6.

3.3. Comparison with previous studies

We compare our results of the pressure broadening and pressure shift coefficients with previous theoretical studies of Refs. [11, 27, 28] and experimental data of Refs. [29, 30]. We present the values separately for purely rotational and rovibrational transitions, respectively in Tables 1, 2 and Tables 3, 4, because of the very recent study of purely rotational lines [11].

First, let us comment on purely rotational transitions. As expected, because of the same method of calculations and applied PES, we obtained the same results as presented in a recent study of Thibault et al. [11]. Small deviations can be explained by some improvements introduced in the present calculations comparing to the previous ones. We slightly changed the propagator's step and increased the number of closed energy levels used in calculations. Moreover, in Ref. [11] the rotational basis was limited to $j = 7$, while in this work we expanded the rotational basis up to $j = 21$. Because our results overlap, for the case of purely rotational lines the reader is referred to [11] for comparison with experimental data and previous calculations.

As γ_0 and δ_0 are the half width at half maximum (HWHM) and shift of Lorentz profile, these values should not be compared with the parameters of the experimental profiles directly. Instead, one should consider a more realistic line-shape function, taking into account speed dependence of the broadening and shift parameters, as well as the velocity-changing collisions. We used our *ab initio* data to simulate a fully synthetic speed dependent quadratic hard collision profile SD_qHCP [22][31][32] and numerically evaluated its HWHM and effective line peak shift (SD_qHCP HWHM and SD_qHCP shift in Tables 1–4).

The experimental data for rovibrational transitions is limited to results for R₁(0) and R₁(1) lines at 77 K of McKellar and Rich [30]. Previous theoretical studies also contain results for P₁(1) line and other temperatures for the pressure broadening coefficient. The values of γ_0 and δ_0 are pre-

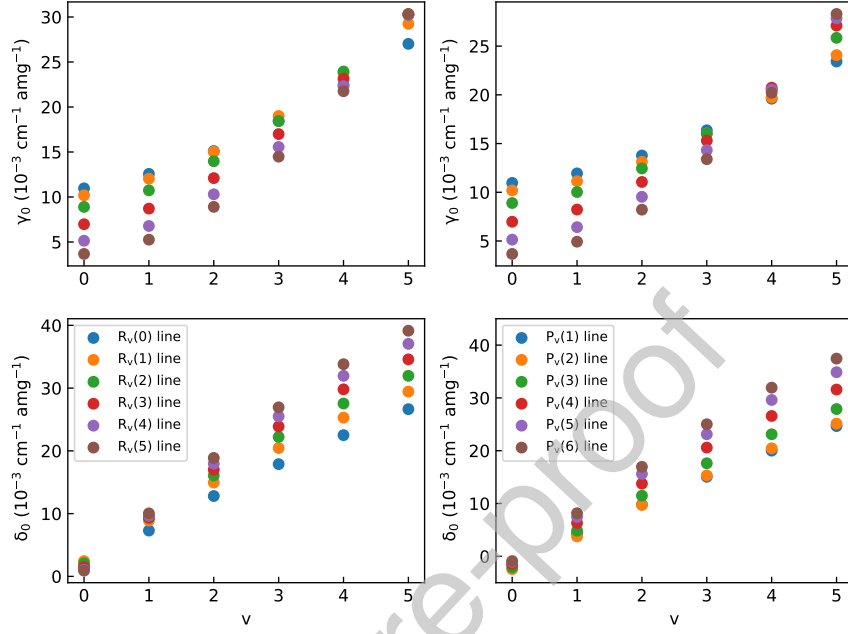


Fig. 5. γ_0 and δ_0 parameters at 296 K for all examined lines in the R and P-branches.

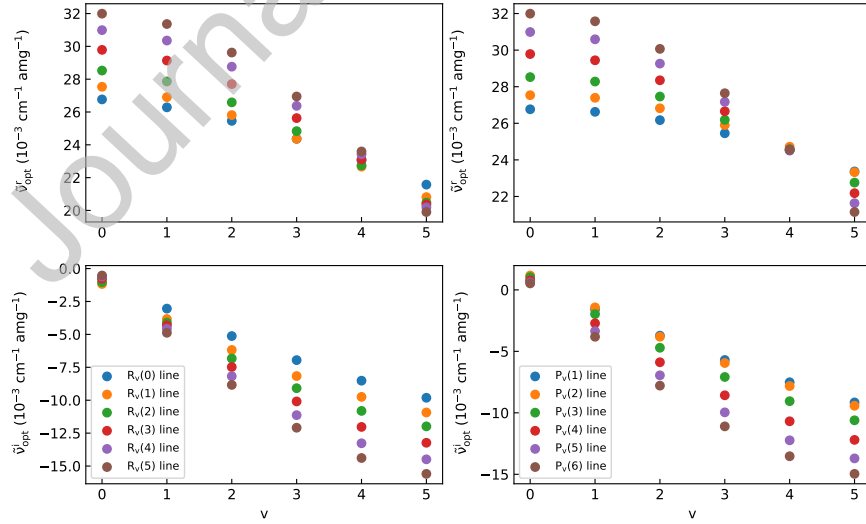


Fig. 6. $\tilde{\nu}_{opt}^r$ and $\tilde{\nu}_{opt}^i$ parameters at 296 K for all examined lines in the R and P-branches.

Table 1

HWHM values determined experimentally and theoretically. Speed-averaged pressure broadening coefficients, γ_0 , are obtained directly from our calculations and the HWHM values are determined numerically from the Speed Dependent quadratic Hard Collision Profile, SD_qHCP, simulated using the line-shape parameters resulting from our calculations. All coefficients are in $10^{-3} \text{ cm}^{-1} \text{ amg}^{-1}$.

T [K]	Purely rotational transitions				exp./calc.
	R ₀ (0)	R ₀ (1)	R ₀ (2)	R ₀ (3)	
77	1.5	2.0	1.2		experiment [29]
	1.81	2.38	2.05	1.38	calculations [11]
	1.81	2.38	2.06	1.38	γ_0 , this work
	1.79	2.36	2.04	1.37	SD _q HCP HWHM, this work
195	5.2	5.1	4.1	3.8	experiment [29]
	6.47	6.26	5.43	4.06	calculations [11]
	6.48	6.27	5.43	4.06	γ_0 , this work
	6.06	6.00	5.24	3.94	SD _q HCP HWHM, this work
296		11	6.8	5.9	experiment [29]
	10.97	10.25	9.0	7.0	calculations [11]
	11.01	10.24	8.94	7.01	γ_0 , this work
	10.00	9.50	8.40	6.65	SD _q HCP HWHM, this work

Table 2

Pressure shift values determined experimentally and theoretically. Speed-averaged pressure-shift coefficients, δ_0 , are obtained directly from our calculations and the line shift values are determined numerically from the SD_qHCP, simulated using the line shape parameters resulting from our calculations. All coefficients are in $10^{-3} \text{ cm}^{-1} \text{ amg}^{-1}$.

T [K]	Purely rotational transitions				exp./calc.
	R ₀ (0)	R ₀ (1)	R ₀ (2)	R ₀ (3)	
77	0.78	0.65	1.11		experiment [29]
	0.74	1.0	0.52	0.22	calculations [11]
	0.74	1.00	0.51	0.21	δ_0 , this work
	0.71	0.98	0.50	0.20	SD _q HCP shift, this work
195	0.98	2.15	1.22	-0.45	experiment [29]
	1.26	1.98	1.46	0.89	calculations [11]
	1.27	1.99	1.46	0.89	δ_0 , this work
	1.19	1.85	1.34	0.82	SD _q HCP shift, this work
296		2.4	2.8	1.8	experiment [29]
	1.45	2.45	2.1	1.5	calculations [11]
	1.45	2.44	2.09	1.47	δ_0 , this work
	1.35	2.23	1.86	1.30	SD _q HCP shift, this work

sented in Table 3 and Table 4, respectively. Our results are in good agreement with radiative close-coupling values of Gustafsson and Frommhold [27], although different PES was used. Despite the semi-classical approach, the difference between our results and those of McQuarrie and Tabisz [28] are also quite small, usually around 20%, but much lower for R₁(1) line. Available experimental data is quite well consistent with our calculations, however, they lie a little beyond the experimental error bars. The experimental HWHM and line shift, as mentioned before, should correspond to the calcu-

Table 3

HWHM values determined experimentally and theoretically in the fundamental band. Speed-averaged pressure broadening coefficients, γ_0 , are obtained directly from our calculations and the HWHM values are determined numerically from the Speed Dependent quadratic Hard Collision Profile, SD_qHCP, simulated using the line-shape parameters resulting from our calculations. All coefficients are in $10^{-3} \text{ cm}^{-1} \text{ amg}^{-1}$.

T [K]	Rovibrational transitions			exp./calc.
	R ₁ (0)	R ₁ (1)	P ₁ (1)	
77	2.8(1)	3.10(15)		experiment [30]
	2.385	2.965	2.06	calculations [27]
	2.39	3.02	2.05	γ_0 , this work
	2.48	3.11	2.05	SD _q HCP HWHM, this work
195	9.49	7.36	9.49	calculations [28]
	7.70	7.65	7.17	γ_0 , this work
	7.49	7.69	6.89	SD _q HCP HWHM, this work
296	14.7	12.2	14.7	calculations [28]
	12.63	12.09	12.00	γ_0 , this work
	12.06	11.91	11.37	SD _q HCP HWHM, this work

Table 4

Pressure shift values in the fundamental band determined experimentally and theoretically. Speed-averaged pressure-shift coefficients, δ_0 , are obtained directly from our calculations and the line shift values are determined numerically from the SD_qHCP. All coefficients are in $10^{-3} \text{ cm}^{-1} \text{ amg}^{-1}$.

T [K]	Rovibrational transitions			exp./calc.
	R ₁ (0)	R ₁ (1)	P ₁ (1)	
77	3.6(1)	4.3(2)		experiment [30]
	3.29	3.78	1.69	calculations [27]
	3.05	3.49	1.47	δ_0 , this work
	2.89	3.34	1.41	SD _q HCP shift, this work

lated effective shift and HWHM of SD_qHCP rather than directly to γ_0 and δ_0 . We note, however, that it is not the case for all the considered transitions. A similar observation was shown in Fig. B.1. in Ref. [11] for R-lines in Lu et al. experiment [29]. Recent measurements of S-lines presented in Fig. 12. Ref. [11] distinctively better agree with the effective values calculated with SD_qHCP than with the γ_0 and δ_0 . For δ_0 the calculations of Ref. [27] are more consistent with the experimental data.

3.4. Centrifugal distortion contribution

It has been demonstrated, that studying collisional perturbation of purely rotational lines of light molecules requires taking into account the influence of the centrifugal distortion [14] and calculating the non-diagonal radial terms of the PES, which couple different rotational levels of the molecule [7, 8, 11]. The role of the centrifugal distortion in the HD-He system for purely rotational lines has been discussed recently in [11], where authors compared

calculations conducted while neglecting and taking into account this effect. Usually it is assumed that the centrifugal distortion for the rovibrational transitions is negligible due to the vibrational dephasing which is supposed to completely dominate this effect. In this subsection, we show, however, that the role of the centrifugal distortion for the rovibrational transitions in the HD-He system cannot be neglected as far as subpercent accuracy is required.

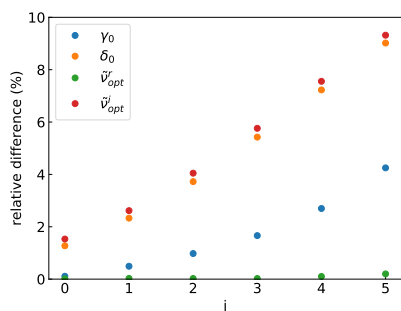


Fig. 7. The relative difference in the values of the collisional line-shape parameters in calculations neglecting and taking into account the centrifugal distortion as a function of initial molecular rotational level j . These relative differences are reported for the studied R lines of the fundamental band at 295 K.

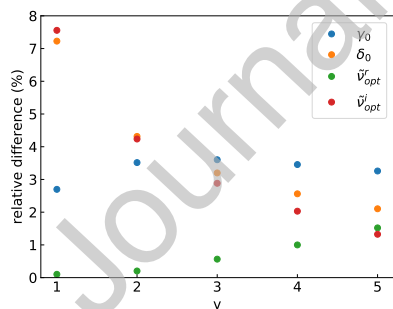


Fig. 8. The relative difference in the values of the collisional line-shape parameters in calculations neglecting, and taking into account the centrifugal distortion as a function of vibrational band $v-0$. These differences are reported for the $R_v(4)$ lines at 295 K. Note, that for $v = 0$, which is not presented here, the error for δ_0 and $\tilde{\nu}_{opt}^i$ is much higher, around 50%, mainly due to their relative small absolute values.

Figures 7 and 8 show the relative difference between the line-shape parameters obtained in calculations neglecting centrifugal distortion and calculations where the effect was taken into account.

They are plotted as a function of the initial rotational number j and vibrational band $v-0$ for chosen representational transitions at 295 K. Figure 7 shows collisional parameters for the R-branch of the fundamental band. As expected, the relative difference for all parameters increases with initial j . The molecular wave functions $\chi_{v,j}(r)$, which are used for calculating the radial terms, differ slightly with j number. The difference between two wavefunction increases with the increasing difference between the initial and final rotational level $j - j'$. In calculations neglecting the centrifugal distortion, radial coupling terms are determined assuming that $\chi_{v,j'}(r) = \chi_{v,j}(r)$ with $j = j' = 0$. Clearly, the error resulting from neglecting the centrifugal distortion should increase with increasing initial rotational level. The error for the fundamental band for δ_0 and $\tilde{\nu}_{opt}^i$ can be as high as 9%, while for γ_0 the error goes up to about 4%. The $\tilde{\nu}_{opt}^r$ is almost insensitive to this effect. Similar behavior applies to other bands and other considered temperatures.

The dependence of collisional parameters on the vibrational band is less monotonical. First, because of the growing role of vibrational dephasing for higher rotational bands, the relative difference resulting from neglecting the centrifugal distortion should decrease with v number. This conclusion applies to δ_0 and $\tilde{\nu}_{opt}^i$ as can be seen in Fig. 8 with few insignificant exceptions for some lines at other temperatures. However, the behavior of γ_0 and $\tilde{\nu}_{opt}^r$ is different. Typically, these differences increase with vibrational level v for lower bands, but they eventually start to drop (see Fig. 8). The same behavior can be observed for $\tilde{\nu}_{opt}^r$, although for lines presented on the graph the difference only increases. A tentative explanation is the presence of competitive effect which is the decreasing of the rotational level spacing with the band. Because of that, for higher bands, more rotational levels must be supplied in the basis set, thus enhancing the error.

As a conclusion, the accuracy of our calculations requires taking into account the centrifugal distortion, especially for higher rotational lines, where the error caused by neglecting centrifugal distortion can reach 9%. All the presented cross-sections and line-shape parameters reported in this paper (and provided in supplementary material [23]) were calculated taking into account the centrifugal distortion.

465 4. Accuracy of calculations

The most important factor that can influence the results of our close-coupling calculations is the accuracy of the PES used. Conservative estimations of the used PES [7] accuracy show that the uncertainty of the interaction energy is not greater than 1% [8]. We multiplied all the radial terms by 1.01 and repeated the calculations of the line-shape parameters for line R(0) in band 1–0 at 3 different temperatures – 77 K, 195 K, and 296 K. The largest error, about 0.45%, was found for the γ_0 coefficient at 77 K.

Other sources of uncertainty are associated with numerical methods of solving the close-coupling equations. The following parameters control the propagator accuracy: the start point of propagation R_{min} , the final point of propagation R_{max} , the number of steps per half-de Broglie wavelength, and the number of asymptotically closed energy levels in the basis (rotational states which energy is higher than the sum of the K.E. and the energy of current molecular rotational state). Figure 9 shows the relative difference between the line-shape parameters resulting from the calculations performed with a different number of asymptotically closed energy levels with respect to the case with 5 asymptotically closed energy levels. It can be seen that the error that comes from using a limited basis in the calculations decreases with an increasing number of closed levels logarithmically. In the present work, we always included 3 closed levels in the basis. The highest relative difference of the line-shape parameters between those results and results for 5 closed levels at temperatures 77 K, 195 K, and 296 K was around 0.003% for the 1–0 R(0) line. This error is negligible comparing to the one resulting from potential uncertainty.

To obtain accurate values of the line-shape parameters, the starting propagation point should lie deep inside the repulsive region of the PES, while the final point should be far outside the turning point for the highest l value associated with J . In the previous studies of the H₂–He system [8] the authors used $R_{min} = 1 a_0$ and $R_{max} = 100 a_0$. The difference resulting from increasing the R_{max} to 200 a_0 is around 0.02% and the difference from decreasing R_{min} is even smaller. In this work, for a similar HD–He system, we put $R_{min} = 0.5 a_0$ and $R_{max} = 200 a_0$. Because of that, the error coming from setting those parameters can be ignored. To choose a proper number of steps per half-de Broglie

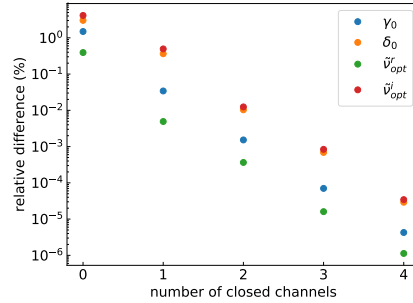


Fig. 9. The relative difference in values of the collisional line-shape parameters in calculations that use from 0 to 4 asymptotically closed energy levels in the basis and calculation that use 5 closed levels. The differences correspond to the R(0) line from 1–0 band at 296 K.

wavelength, we conducted calculations of GSXS for a series of increasing steps. For each energy, we selected steps that guarantee at least 0.1% accuracy, however, for most energies the accuracy was higher. We then repeated calculations of the line-shape parameters for R(0) 1–0 line with 2 times higher step value. The largest error, 0.06%, occurred for δ_0 at 77 K.

After taking into account all the factors, we concluded that the most important influence on the accuracy of the calculations comes from the uncertainty of the PES. The total uncertainty of our calculations is estimated at 0.6%.

5. Conclusion

The pressure broadening, pressure shift, as well as the real and imaginary part of the complex Dicke parameter for HD in helium bath for 12 purely rotational and 60 rovibrational lines were calculated. We obtained the line-shape parameters γ_0 , δ_0 , $\tilde{\nu}_{opt}^r$ and $\tilde{\nu}_{opt}^i$ at 30 temperatures ranging from 5 to 2000 K. We examined the centrifugal distortion contribution to the line-shape parameters of rovibrational transitions and concluded, that for accurate calculations it is important to take it into account. There is a necessity of more accurate experimental studies of the collisional line-shape effects to validate results of reported calculations.

6. Acknowledgment

KS and MG contributions are supported by the *A next-generation world-wide quantum sensor net-*

work with optical atomic clocks project carried out within the TEAM IV Programme of the Foundation for Polish Science conanced by the European Union under the European Regional Development Fund. HJ and NS contribution is supported by the National Science Centre in Poland through project no. 2018/31/B/ST2/00720. PW contribution is supported by the National Science Centre in Poland through project no. 2019/35/B/ST2/01118. The project is supported by the French-Polish PHC Polonium program (project 42769ZK for the French part). The project is co-financed by the Polish National Agency for Academic Exchange under the PHC Polonium program (dec.PPN/X/PS/318/2018).

- [1] E. Miller-Ricci, D. Sasselov, S. Seager, The Atmospheric Signatures of Super-Earths: How to Distinguish Between Hydrogen-Rich and Hydrogen-Poor Atmospheres, *The Astrophysical Journal* 690. doi:10.1088/0004-637X/690/2/1056.
- [2] H. Feuchtgruber, E. Lellouch, G. Orton, T. Graauw, B. Vandembussche, B. Swinyard, R. Moreno, C. Jarchow, F. Billebaud, T. Cavalié, S. Sidher, P. Hartogh, The D/H ratio in the atmospheres of Uranus and Neptune from Herschel PACS observations, *Astronomy and Astrophysics* 551. doi:10.1051/0004-6361/201220857.
- [3] J. Fortney, T. Robinson, S. Domagal-Goldman, A. Delgenio, I. Gordon, E. Gharib-Nezhad, N. Lewis, C. Sousa-Silva, V. Airapetian, B. Drouin, R. Hargreaves, X. Huang, T. Karman, R. Ramirez, G. Rieker, J. Tennyson, R. Wordsworth, S. Yurchenko, A. Johnson, L. Close, The Need for Laboratory Measurements and Ab Initio Studies to Aid Understanding of Exoplanetary Atmospheres, arXiv.org.
- [4] W. Smith, C. Conner, J. Simon, W. Schempp, W. Macy, The H₂ 4-0 S(0,1, and 2) quadrupole features in Jupiter, *Icarus*; (USA) 81. doi:10.1016/0019-1035(89)90062-6.
- [5] K. Baines, M. Mickelson, L. Larson, D. Ferguson, The Abundances of Methane and Ortho/Para Hydrogen on Uranus and Neptune: Implications of New Laboratory 4-0 H₂ Quadrupole Line Parameters, *Icarus* 114. doi:10.1006/icar.1995.1065.
- [6] F. Thibault, P. Wcisło, R. Ciuryło, A test of H₂-He potential energy surfaces, *The European Physical Journal D* 70. doi:10.1140/epjd/e2016-70114-9.
- [7] F. Thibault, K. Patkowski, P. Żuchowski, H. Józwiak, R. Ciuryło, P. Wcisło, Rovibrational line-shape parameters for H₂ in He and new H₂-He potential energy surface, *Journal of Quantitative Spectroscopy and Radiative Transfer* 202. doi:10.1016/j.jqsrt.2017.08.014.
- [8] H. Józwiak, F. Thibault, N. Stolarczyk, P. Wcisło, Ab initio line-shape calculations for the S and O branches of H₂ perturbed by He, *Journal of Quantitative Spectroscopy and Radiative Transfer* 219. doi:10.1016/j.jqsrt.2018.08.023.
- [9] M. Słowiński, F. Thibault, Y. Tan, J. Wang, A.-W. Liu, S.-M. Hu, S. Kassı, A. Campargue, M. Konefał, H. Józwiak, K. Patkowski, P. Żuchowski, R. Ciuryło, D. Lisak, P. Wcisło, H₂-He collisions: Ab initio theory meets cavity-enhanced spectra, *Phys. Rev. A* doi:10.1103/PhysRevA.101.052705.
- [10] P. Wcisło, et al., The first comprehensive dataset of beyond-Voigt line-shape parameters from ab initio quantum scattering calculations for the HITRAN database: He-perturbed H₂ case study, in preparation.
- [11] F. Thibault, R. Martínez, D. Bermejo, P. Wcisło, Line-shape parameters for the first rotational lines of HD in He, *Molecular Astrophysics* doi:10.1016/j.molap.2020.100063.
- [12] B. Bakr, D. Smith, K. Patkowski, Highly accurate potential energy surface for the He-H₂ dimer, *The Journal of Chemical Physics* 139. doi:10.1063/1.4824299.
- [13] H. Józwiak, M. Gancewski, K. Stankiewicz, P. Wcisło, BIGOS computer code, to be published.
- [14] M. Dubernet, P. Tuckey, Raman Q and S line broadening and shifting coefficients: Some commonly used assumptions revisited, *Chemical Physics Letters* 300. doi:10.1016/S0009-2614(98)01334-7.
- [15] R. Martínez, D. Bermejo, F. Thibault, P. Wcisło, Testing the ab initio quantum-scattering calculations for the D₂-He benchmark system with stimulated Raman spectroscopy, *Journal of Raman Spectroscopy* 49. doi:10.1002/jrs.5391.
- [16] A. Arthur, A. Dalgarno, The Theory of Scattering by a Rigid Rotator, *Proceedings of The Royal Society A: Mathematical, Physical and Engineering Sciences* 256. doi:10.1098/rspa.1960.0125.
- [17] D. Flower, *Molecular Collisions in the Interstellar Medium*, Cambridge University Press, 2007. doi:10.1017/cbo9780511536229.
- [18] B. Johnson, Multichannel log-derivative method for scattering calculations, *J. Comput. Phys.*, v. 13, no. 3, pp. 445-449 13. doi:10.1016/0021-9991(73)90049-1.
- [19] L. Monchick, L. Hunter, Diatomic-diatom molecular collision integrals for pressure broadening and Dicke narrowing - A generalization of Hess's theory, *Chemical Physics* 85. doi:10.1063/1.451277.
- [20] J. Schaefer, L. Monchick, Line broadening of HD immersed in He and H₂ gas, *Astronomy and Astrophysics* 265.
- [21] L. Demeio, S. Green, L. Monchick, Effects of velocity changing collisions on line shapes of HF in Ar, *Chemical Physics* 102. doi:10.1063/1.468864.
- [22] P. Wcisło, F. Thibault, M. Zaborowski, S. Wójtewicz, A. Cygan, G. Kowzan, P. Masłowski, J. Komasa, M. Puchalski, K. Pachucki, R. Ciuryło, D. Lisak, Accurate deuterium spectroscopy for fundamental studies, *Journal of Quantitative Spectroscopy and Radiative Transfer* 213. doi:10.1016/j.jqsrt.2018.04.011.
- [23] K. Stankiewicz, H. Józwiak, M. Gancewski, N. Stolarczyk, F. Thibault, P. Wcisło, Supplementary material.
- [24] A. Ben-Reuven, Symmetry Considerations in Pressure-Broadening Theory, *Physical Review* 141. doi:10.1103/PhysRev.141.34.
- [25] R. Wehr, R. Ciuryło, A. Vitcu, F. Thibault, J. Drummond, A. May, Dicke-narrowed spectral line shapes of CO in Ar: Experimental results and a revised interpretation, *Journal of Molecular Spectroscopy* 235. doi:10.1016/j.jms.2005.10.009.
- [26] N. Stolarczyk, F. Thibault, H. Cybulski, H. Józwiak, G. Kowzan, B. Vispoel, I. Gordon, L. Rothman, R. Gamache, P. Wcisło, Evaluation of different parameterizations of temperature dependences of the line-shape parameters based on ab initio calculations: Case study for the HITRAN database, *Journal of Quantitative Spectroscopy and Radiative Transfer* 213. doi:10.1016/j.jqsrt.2018.04.011.

- tative Spectroscopy and Radiative Transfer 240. doi:
<https://doi.org/10.1016/j.jqsrt.2019.106676>.
- 675 [27] M. Gustafsson, L. Frommhold, The HD-He complex:
Interaction-induced dipole surface and infrared absorp-
tion spectra, The Journal of Chemical Physics 115.
doi:10.1063/1.1396851.
- 680 [28] B. McQuarrie, G. Tabisz, Collisional interference in
the infrared spectrum of HD: calculation of the line
shape of vibrorotational transitions for HD-He, Jour-
nal of Molecular Liquids 70 (2), diatomic Molecules in
Dense Non-Polar Solvents. doi:[https://doi.org/10.1016/0167-7322\(96\)00965-8](https://doi.org/10.1016/0167-7322(96)00965-8).
- 685 [29] Z. Lu, G. Tabisz, L. Ulivi, Temperature dependence of
the pure rotational band of HD: Interference, widths,
and shifts, Physical review. A 47. doi:10.1103/
PhysRevA.47.1159.
- 690 [30] A. McKellar, N. Rich, Interference effects in the spec-
trum of HD: II. The fundamental band for HD-rare
gas mixtures, Canadian Journal of Physics 62. doi:
10.1139/p84-211.
- [31] M. Nelkin, A. Ghatak, Simple Binary Collision Model
for Van Hove's $G_s(r,t)$, Physical Review 135. doi:10.
1103/PhysRev.135.A4.
- 695 [32] S. G. Rautian, I. I. Sobel'man, The effect of collisions
on the Doppler broadening of spectral lines, Phys. Usp.
9 (5). doi:10.1070/PU1967v009n05ABEH003212.

CRedit authorship contribution statement

Kamil Stankiewicz: Conceptualization , Software, Validation, Investigation, Writing - Original Draft, Writing - Review & Editing, Visualization
Hubert Józwiak: Conceptualization, Methodology, Software, Validation, Writing - Original Draft, Writing - Review & Editing
Maciej Gancewski: Software, Investigation, Writing - Original Draft, Writing - Review & Editing
Nikodem Stolarczyk: Software, Investigation, Writing - Original Draft, Writing - Review & Editing
Franck Thibault: Conceptualization, Methodology, Software, Validation, Resources, Writing - Review & Editing
Piotr Wcisło: Conceptualization, Methodology, Writing - Review & Editing, Supervision, Project administration, Funding acquisition

Declaration of Competing Interests

The authors declare that they have no known competing financial interests or personal relationships that could have appeared to influence the work reported in this paper.